Scattering of Charged Particles by Helium Atoms*

Victor Franco
Physics Department, Brooklyn College of the City University of New York, Brooklyn, New York 11210†
and
University of California, Los Alamos Scientific Laboratory, Los Alamos, New Mexico 87544
(Received 15 January 1970)

Elastic and inelastic scattering of charged particles by helium atoms is analyzed in the Glauber approximation. Applications are made to the differential cross sections for electron-helium elastic scattering, and the predictions are compared with the first Born approximation and with measurements between 100 and 500 eV. At small momentum transfers the calculated intensities for elastic scattering are significantly greater than those obtained from the Born approximation.

The predictions of the Glauber approximation for *elastic* scattering of charged particles by atomic hydrogen[1] have been confirmed by recent electron-hydrogen measurements.[2] A detailed application of the theory to atomic hydrogen *excitation* by electron impact[3] has very recently shown these predictions also to be in remarkably good agreement with the measurements, even for energies substantially below 100 eV. The success of the theory for describing collisions with atomic hydrogen leads naturally to the question of its applicability to scattering by more complex targets. We present here the corresponding theory for scattering of charged particles by helium atoms, together with applications to electron-helium elastic scattering and comparisons with recent measurements.[4,5]

The basic features and expected range of validity of the theory are outlined in Ref. 1 and given in more detail in works cited therein. The basic method by which the theory is applied to scattering by arbitrary atomic systems is a simple generalization of the method used in Ref. 1 for scattering by atomic hydrogen. In the latter case it was necessary to evaluate a five-dimensional integral. For scattering by helium atoms the theory leads to an eight-dimensional integral. In general, if no additional approximations are made in the theory, the analysis of scattering by a Z-electron atom leads to the evaluation of a $(3Z+2)$-dimensional integral.

As in Ref. 1 we treat the target nucleus as being infinitely heavy and neglect exchange effects. The amplitude $F_{fi}(\vec{q})$ for collisions, in which a helium atom undergoes a transition from an initial state i with wave function φ_i to a final state f with wave function φ_f and the incident particle imparts a momentum $\hbar\vec{q}$ to the target, is very similar in form to the amplitude for corresponding collisions involving atomic hydrogen.[1] Let the origin of coordinates be placed at the helium nucleus, and let $\vec{b}$ denote the impact-parameter vector relative to the origin. If $\vec{r}_1$, $\vec{r}_2$ denote the position vectors of the target electrons, the amplitude for scattering of a particle of momentum $\hbar k$ by helium takes the form

$$F_{fi}(\vec{q}) = (ik/2\pi)\int \varphi_f^*(\vec{r}_1,\vec{r}_2)\Gamma(\vec{b},\vec{r}_1,\vec{r}_2)\varphi_i(\vec{r}_1,\vec{r}_2) \times \exp(i\vec{q}\cdot\vec{b})\, d^2b\, d\vec{r}_1\, d\vec{r}_2 , \quad (1)$$

where the two-dimensional integration over impact-parameter vectors is over a plane perpendicular to the direction of the incident beam. Equation (1), in which an eight-dimensional integral appears, is a simple extension of Eq. (1) of Ref. 1 to two-electron atoms. As in the case for scattering by atomic hydrogen, the function Γ itself depends upon an integral, along the direction of the incident beam, of the instantaneous potential V between the incident particle and the target. Since the potential between the incident particle and the target protons will not be neglected, and since Γ is not a linear function of V, the theory explicitly treats the effects of the presence of the nucleus. Specifically, if $\vec{r}=\vec{b}+\vec{\zeta}$ is the position vector of the incident electron, the function Γ may be expressed as

$$\Gamma(\vec{b},\vec{r}_1,\vec{r}_2) = 1-\exp[(-i/\hbar v)\int_{-\infty}^{\infty} V(\vec{r},\vec{r}_1,\vec{r}_2)\, d\zeta]$$

$$= 1-\exp[(-iZe^2/\hbar v) \times \int_{-\infty}^{\infty}(2r^{-1}-|\vec{r}-\vec{r}_1|^{-1}-|\vec{r}-\vec{r}_2|^{-1})\, d\zeta] ,$$

where Ze is the charge of the incident particle and v its velocity. If we write $\vec{r}_1=\vec{s}_1+\vec{z}_1$ and $\vec{r}_2=\vec{s}_2+\vec{z}_2$, where $\vec{s}_1$ and $\vec{s}_2$ are the projections of $\vec{r}_1$ and $\vec{r}_2$, respectively, onto the plane of impact parameters, Γ may be expressed as

$$\Gamma(\vec{b},\vec{r}_1,\vec{r}_2)$$

$$=1-\exp[(-2iZe^2/\hbar v)\ln(|\vec{b}-\vec{s}_1||\vec{b}-\vec{s}_2|/b^2)]. \quad (2)$$

The integral [(1)] may be reduced to

$$F_{fi}(q)=ik\int J_0(qb)\,\varphi_f^*(\vec{r}_1,\vec{r}_2)\times[1-(|\vec{b}-\vec{s}_1||\vec{b}-\vec{s}_2|/b^2)^{-2inZ}]\times\varphi_i(\vec{r}_1,\vec{r}_2)b\,db\,dz_1\,dz_2\,d^2s_1\,d^2s_2\,, \quad (3)$$

where the integration with respect to impact parameters b is over the interval $(0,\infty)$ and where $n=e^2/\hbar v$. If we assume that the wave functions φ_i and φ_f possess azimuthal symmetry about the direction of the incident beam and if we transform the integration variables b, s_1, s_2 to spherical coordinates r,θ,ϕ, two additional integrations may be performed, namely the angular integrations corresponding to d^2s_1 and d^2s_2. The result is

$$F_{fi}(q)=4\pi^2ik\int_0^{\pi/2}\int_0^{\pi/2}J_0(qr\cos\theta)\,\varphi_f^*A(\theta,\phi)\,\varphi_i\,r^5\times\sin^3\theta\cos\theta\sin\phi\cos\phi\,dr\,d\theta\,d\phi\,dz_1\,dz_2\,, \quad (4)$$

where

$$A(\theta,\phi)=1-(4\tan^2\theta\sin\phi\cos\phi)^{-Zin}(xy)^{-1+Zin}\times[(x^2-1)(y^2-1)]^{1/2-Zin}\times F(\tfrac{1}{2}-\tfrac{1}{2}Zin,1-\tfrac{1}{2}Zin;1;x^{-2})\times F(\tfrac{1}{2}-\tfrac{1}{2}Zin,1+\tfrac{1}{2}Zin;1;y^{-2})\,, \quad (5)$$

in which $y=\csc2\theta\sec\phi(1-\sin^2\theta\sin^2\phi)$,

$x=\csc2\theta\csc\phi(1-\sin^2\theta\cos^2\phi)$.

The integration limits refer to the angular integrations, and F is the hypergeometric function.

Cross sections for both *elastic and inelastic* collisions may be explicitly calculated by means of Eq. (4). As an example, we consider elastic scattering of electrons by helium in its ground state. For this case $Z=-1$ and $\varphi_f=\varphi_i$. There exist a variety of ground-state wave functions which may be chosen. We have performed the calculations for a number of such wave functions. As an illustration, we consider the wave function[6]

$$\varphi_i(\vec{r}_1,\vec{r}_2)=(N^2/\pi a_0^3)[\exp(-Z_1r_1/a_0)+c\exp(-2Z_1r_1/a_0)]\times[\exp(-Z_1r_2/a_0)+c\exp(-2Z_1r_2/a_0)]\,, \quad (6)$$

with $N=1.484$, $Z_1=1.456$, and $c=0.6$, and where a_0 is the first Bohr radius. Upon performing the z_1 and z_2 integrations, Eq. (4) becomes

$$F_{ii}(q)=(16N^4ik/a_0^6)\int_0^{\pi/2}\int_0^{\pi/2}\int_0^{\infty}J_0(qr\cos\theta)A(\theta,\phi)\times B(r,\theta,\phi)r^7\sin^5\theta\cos\theta\sin^2\phi\cos^2\phi\,dr\,d\theta\,d\phi\,, \quad (7)$$

where

$$B(r,\theta,\phi)=\left[K_1\left(\frac{2Z_1r\sin\theta\cos\phi}{a_0}\right)+2cK_1\left(\frac{3Z_1r\sin\theta\cos\phi}{a_0}\right)+c^2K_1\left(\frac{4Z_1r\sin\theta\cos\phi}{a_0}\right)\right]\times\left[K_1\left(\frac{2Z_1r\sin\theta\sin\phi}{a_0}\right)+2cK_1\left(\frac{3Z_1r\sin\theta\sin\phi}{a_0}\right)+c^2K_1\left(\frac{4Z_1r\sin\theta\sin\phi}{a_0}\right)\right]. \quad (8)$$

Equation (7) is a three-dimensional integral which may be evaluated numerically. The differential cross section is obtained by means of the relation

$$d\sigma/d\Omega=|F_{ii}(q)|^2\,. \quad (9)$$

For comparison we have also calculated the elastic scattering amplitude $F_B(q)$ in the first Born approximation (FBA) using the wave function [(6)]. The result is

$$F_B(q)=\frac{4N^2a_0}{Z_1^3}\left(\frac{(a_0q)^2+8Z_1^2}{[(a_0q)^2+4Z_1^2]^2}+\frac{16c}{27}\times\frac{(a_0q)^2+18Z_1^2}{[(a_0q)^2+9Z_1^2]^2}+\frac{c^2}{8}\frac{(a_0q)^2+32Z_1^2}{[(a_0q)^2+16Z_1^2]^2}\right). \quad (10)$$

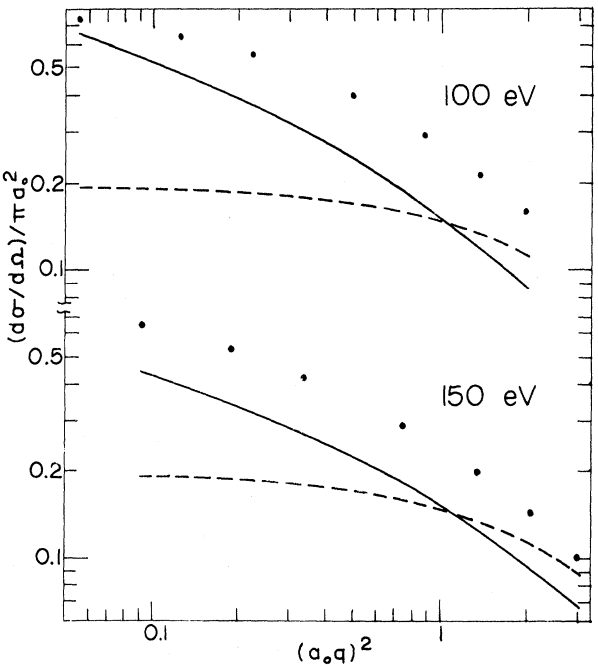

FIG. 1. Differential cross sections for electron-helium elastic scattering at 100 and 150 eV. The measurements were made by Vriens *et al.* and Chamberlain *et al.* (Ref. 4). The solid curves are obtained from Eq. (7) and the dashed curves from Eq. (10).

We have calculated the differential cross sections that result from the amplitude [(7)] and the Born amplitude [(10)] for electron energies between 100 and 500 eV, and we have compared the predictions with recent measurements.[4,5] In Fig. 1 we compare the calculated intensities with data at 100 and 150 eV. Both the shapes and the magnitudes of the FBA intensities are rather poor. On the other hand, the shapes of the intensities obtained from Eq. (7) are quite good and the magnitudes are within approximately 35% of the measurements. In Fig. 2 we compare the calculated intensities with data at 200 and 300 eV. Again the shapes and magnitudes of the FBA intensities are poor, whereas the shapes of the intensities obtained from Eq. (7) are excellent and the magnitudes are within approximately 25% of the measured values. In Fig. 3 we compare the calculated intensities with data at 400 and 500 eV. We note that the present theory is in good agreement with the measurements, whereas the FBA is still much too low at small momentum transfers. The intensities obtained from Eq. (7) are within approximately 20% of the data.

We note from Figs. 1–3 that the shapes of the differential cross sections calculated from Eq. (4) reproduce the shapes of the corresponding measurements quite well, whereas at all energies the shapes obtained from the FBA are rather poor. A renormalization of the data could, of course, result in even better agreement between the measurements and the magnitudes of the calculated intensities. Given the basic approximations of the theory, the only assumption we have made concerned the choice of wave function φ_i. It is conceivable that a more sophisticated ground-state wave function could also improve the agreement of the present calculations with the data.

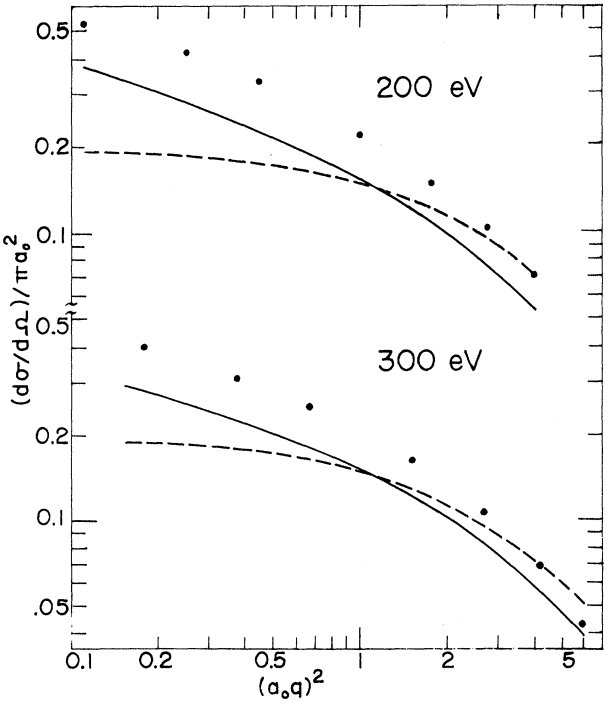

FIG. 2. Same as Fig. 1, but for energies of 200 and 300 eV.

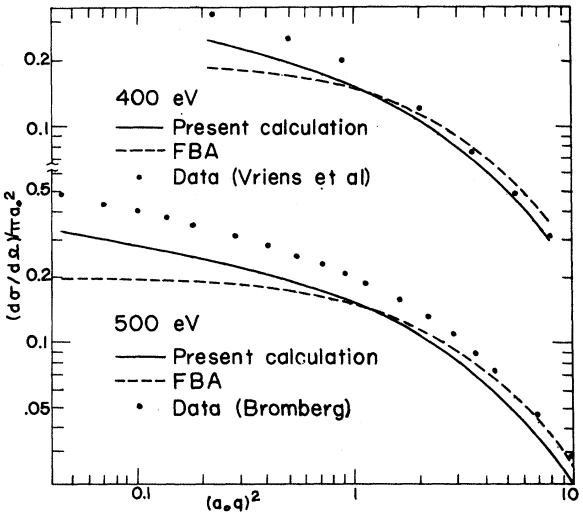

FIG. 3. Same as Fig. 1, but for energies of 400 and 500 eV, with the measurements at 400 eV by Vriens *et al.* and Chamberlain *et al.* (Ref. 4) and those at 500 eV by Bromberg (Ref. 5).

Inspection of Figs. 1–3 shows that for the range of momentum transfers considered, the present theory and the Born theory approach each other as the incident energy is increased. However, the approach is rather slow and the differences between the two theories are even more significant at momentum transfers less than and greater than those shown in the figures. The two theoretical curves intersect at momentum transfers such that the area between the two curves to the left of the intersection is approximately equal to the corresponding area to the right of the intersection. This property results in a very small difference between the integrated elastic scattering cross sections computed from Eqs. (7) and (10). This effect is similar to that for electron-hydrogen scattering.[1] Consequently, comparison of calculated *integrated* cross sections does not reveal the significant differences between the present theory and the Born theory.

The author is grateful to Dr. W. R. Gibbs and Dr. M. Rich for their help in obtaining numerical results.

*Supported in part by the U. S. Atomic Energy Commission.

†Present address.

[1]V. Franco, Phys. Rev. Letters 20, 709 (1968).

[2]H. Tai, P. J. Teubner, and R. H. Bassel, Phys. Rev. Letters 22, 1415 (1969); and 23, 453(E) (1969).

[3]H. Tai, R. H. Bassel, E. Gerjuoy, and V. Franco this issue, Phys. Rev. A 1, 1819 (1970).

[4]L. Vriens, C. E. Kuyatt, and S. R. Mielczarek, Phys. Rev. 170, 163 (1968); G. E. Chamberlain, S. R. Mielczarek, and C. E. Kuyatt, in *Proceedings of the Sixth International Conference on the Physics of Electronic and Atomic Collisions, Boston, 28 July-2 August*, 1969 (M. I. T. Press, Cambridge, Mass., 1969), p. 341; G. E. Chamberlain (private communication).

[5]J. P. Bromberg, J. Chem. Phys. 50, 3906 (1969).

[6]N. F. Mott and H. S. W. Massey, *The Theory of Atomic Collisions* (Oxford U. P., New York, 1965), p. 456.

PHYSICAL REVIEW A VOLUME 1, NUMBER 6 JUNE 1970

Spin-Lattice Relaxation of Liquid He^3 and He^3-He^4 Mixtures*

E. Philip Horvitz†

Rice University, Houston, Texas 77001

(Received 22 September 1969; revised manuscript received 2 February 1970).

The relaxation times T_1 and T_2 of He^3 nuclei in pure liquid He^3 and in liquid He^3-He^4 mixtures have been measured in the temperature range $0.9°K<T<2.6°K$. Reproducible relaxation times longer than those previously reported have been obtained by employing an extensive cleaning procedure. The Pyrex sample chamber and filling capillary were repeatedly cleaned in the presence of several mm of pure He^4 by heating the glass to almost melting and, at the same time, touching the glass surface with a Tesla coil. This coil creates a high-frequency discharge which drives absorbed gases off the wall. T_1 for pure He^3 was found to have the value and the temperature dependence predicted by the modified Bloembergen-Purcell-Pound theory to within ±3%. T_1 is proportional to the diffusion coefficient, and increases from 350 sec at 1.0° K to 450 sec at 1.8° K. T_2 was found to be approximately equal to T_1. These long relaxation times were significantly shortened by contamination of the clean chamber with air or by inadequate purification of the He^3 sample. Since the work on pure He^3 showed that wall effects could be minimized by cleaning, it was considered of interest to measure T_1 in He^3-He^4 mixtures. The relaxation times of a 33% He^3 solution were determined in an extensively cleaned system. Above the λ point, T_1 is about 50% greater than for pure He^3, while just below this temperature it increases sharply by about 15%. Measurements of T_1 of other mixtures were made in partially cleaned systems. The results were affected by wall relaxation and bulk impurities. Some conclusions about T_1 are drawn from these data.

INTRODUCTION

The spin-lattice relaxation times of liquid He^3 and He^3 - He^4 mixtures have been studied by several investigators.[1-7] They found the relaxation to be affected by impurities in suspension and on the wall. As a result of these impurities the relaxation times were often found to have the following erratic characteristics. (i) The results were not reproducible. (ii) The spread in T_1 values was greater than could be accounted for. (iii) Sometimes the magnetization approached equilibrium as a compound recovery with two relaxation times.[6] An explanation for this is presented in the Appendix. (iv) T_2 was found to be shorter than T_1.[1,8]

This article reports the results of research that shows that the impurity and wall effects are significantly reduced by employing an extensive cleaning procedure.[9] As a result of this cleaning procedure, reproducible spin-lattice relaxation times have been obtained for pure He^3. The relaxation times are longer than those previously reported and have the value and temperature dependence predicted by the modified BPP theory. T_1 is proportional to the diffusion coefficient and increases from 350 sec at 1.0 °K to 450 sec at 1.8 °K. The longest relaxation times previously obtained were by Romer,[2] who found T_1 to be 310 sec at 1.0 °K and 350 sec at 1.8 °K.

The relaxation times of a 33% He^3 solution were measured in a clean system. Above the λ temperature, T_1 is about 50% greater than for pure He^3. Below this temperature T_1 increases sharply by about 15%. This is expected in terms of the BPP theory since the diffusion coefficient